Turkish Journal of Electrical Engineering & Computer Sciences

http://journals.tubitak.gov.tr/elektrik/

Research Article

Turk J Elec Eng & Comp Sci
(2017) 25: 965 – 975

doi:10.3906/elk-1510-89

A novel direct torque control using second order continuous sliding mode of a doubly fed induction generator for a wind energy conversion system

Zinelaabidine BOUDJEMA[1,*], **Rachid TALEB**[1], **Youcef DJERIRI**[2], **Adil YAHDOU**[1]
[1]Department of Electrical Engineering, Faculty of Technology, Hassiba Benbouali University, Chlef, Algeria
[2]Department of Electrical Engineering, Faculty of Technology, Djillali Liabes University, Sidi Bel-Abbes, Algeria

Received: 12.10.2015 • **Accepted/Published Online:** 12.03.2016 • **Final Version:** 10.04.2017

Abstract: In this paper a new robust direct torque control strategy based on second order continuous sliding mode and space vector modulation of a doubly fed induction generator integrated in a wind energy conversion system is presented. The conventional direct torque control (C-DTC) with hysteresis regulators has significant flux and torque ripples at steady-state operation and also the switching frequency varies in a wide range. The proposed DTC technique based on second order continuous sliding mode control reduces flux, current, and torque ripples. It also narrows down the switching frequency variations in induction machine control. Two different sliding surfaces such as flux and torque sliding surfaces are used to control them. The error between reference and actual values are driven to respective sliding surfaces where the error is enforced to zero. Simulation results show the effectiveness of the proposed direct torque control strategy comparatively to the C-DTC one.

Key words: Doubly fed induction generator, wind turbine system, direct torque control, second order continuous sliding mode

1. Introduction

In recent years, wind energy technology has drawn much attention from research groups and industry. This has been confirmed by the large number of research papers published over this period of time. Today the variable speed wind turbine system (WTS) based on a doubly fed induction generator (DFIG) is the most used in onshore wind farms [1]. The principal advantage of the DFIG is that the rotor side converter (RSC) is only sized for 30% of rated power compared to other generators used in variable speed WTSs. Consequently, the cost of the converter becomes less [2].

Stator field oriented control using proportional-integral (PI) controllers is the conventional control scheme used for DFIG-based WTS [3,4]. In this control scheme, the decoupling between d-axis and q-axis current is achieved with feedforward compensation, and thus the DFIG model becomes less difficult and PI controllers can be used. Nevertheless, this control structure is strongly dependent on machine parameters, uses multiple loops, and requires much regulation effort to guarantee structure stability over the total velocity range [5].

In order to overcome the drawbacks of the vector control, direct torque control (DTC) has been presented [3,6]. In the conventional direct torque control (C-DTC), torque and flux can be directly controlled by using switching table and hysteresis controllers. Nevertheless, a few disadvantages limit the use of these controllers,

*Correspondence: boudjemaa1983@yahoo.fr

such as variable switching frequency and torque ripple [7,8]. In many research papers on DTC, these adverse effects are reduced by using the SVM scheme; however, the robustness of the control is sacrificed [9,10].

Recently the sliding mode control (SMC) methodology has been widely used for robust control of nonlinear systems. SMC, based on the theory of variable structure systems, has attracted a lot of research on control systems for the last two decades. It achieves robust control by adding a discontinuous control signal across the sliding surface, satisfying the sliding condition. Nevertheless, the standard SMC has an important disadvantage, which is the chattering phenomenon caused by the discontinuous control signal. To resolve this problem, several modifications to the usual control law have been proposed. In most cases, the boundary layer approach is applied [11].

Some useful solutions for sliding mode DTC with less torque and flux ripples used in induction motor drives were described in [12,13]. In [14], the authors proposed the use of a DTC with second order sliding mode (SOSM) controllers applied to the induction motor drive.

Newly developed, SOSM generalizes the essential sliding mode scheme that acts on the second order time derivatives of the structure variation since the constraint instead of influencing the initial variation derivative as it occurs in standard sliding modes [15]. Some such controllers were reported in the literature [16–19].

In order to elaborate a robust DTC without torque and flux ripples and with lower chattering phenomenon, in this paper we propose to use a second order continuous sliding mode direct torque control (SOCSM-DTC) for a DFIG drive integrated in a WTS. The proposed strategy takes into account the nonlinear nature of the WTS behavior, the flexibility of the drive train, and the turbulent nature of the wind. Suggested by Levant in [20], this control strategy presents attractive features such as robustness to parametric uncertainties of the DFIG and also presents robustness with respect to internal and external disturbances and model uncertainties, finite-time convergence, and reduced chattering.

This paper presents the fundamental aspects of the SOCSM-DTC and presents pertinent simulation results for a DFIG drive. The proposed strategy is compared with a C-DTC. The original contribution of this paper is the application of the proposed strategy to control the torque and flux of DFIG drives supplied by a pulse width modulation (PWM) inverter. The simulation results validate that the SOCSM-DTC has very robust behavior, like conventional SMC, and it works without remarkable steady-state chattering. This represents a novel robust and ripple-free DTC method for DFIG drive control.

2. The DFIG model

In the literature, the Park model of the DFIG is largely used [21,22]. The equations of voltages and fluxes for the DFIG stator and rotor in the Park reference frame are given as follows.

$$\begin{cases} V_{ds} = R_s I_{ds} + \frac{d}{dt}\psi_{ds} - \omega_s \psi_{qs} \\ V_{qs} = R_s I_{qs} + \frac{d}{dt}\psi_{qs} + \omega_s \psi_{ds} \\ V_{dr} = R_r I_{dr} + \frac{d}{dt}\psi_{dr} - \omega_r \psi_{qr} \\ V_{qr} = R_r I_{qr} + \frac{d}{dt}\psi_{qr} + \omega_r \psi_{dr} \end{cases}, \begin{cases} \psi_{ds} = L_s I_{ds} + M I_{dr} \\ \psi_{qs} = L_s I_{qs} + M I_{qr} \\ \psi_{dr} = L_r I_{dr} + M I_{ds} \\ \psi_{qr} = L_r I_{qr} + M I_{qs} \end{cases} \tag{1}$$

V_{ds}, V_{qs}, V_{dr}, and V_{qr} are the two-phase stator and rotor voltages; I_{ds}, I_{qs}, I_{dr}, and I_{qr} are the two-phase stator and rotor currents; ψ_{ds}, ψ_{qs}, ψ_{dr}, and ψ_{qr} are the two-phase stator and rotor fluxes; R_s and R_r are respectively the resistances of the rotor and stator windings; and L_s, L_r, and M are respectively the inductance on the stator, the inductance on the rotor, and the mutual inductance between two coils.

The stator and rotor angular velocities are linked by the following relation: $\omega_s = \omega + \omega_r$. ω_s is the electrical pulsation of the stator and ω_r is the rotor one, while ω is the mechanical pulsation of the DFIG.

The electrical model of the DFIG is completed by the following mechanical equation:

$$C_{em} = C_r + J \cdot \frac{d\Omega}{dt} + f \cdot \Omega \tag{2}$$

Here, the electromagnetic torque C_{em} can be written as follows:

$$C_{em} = \frac{3}{2} p \frac{M}{L_s} (\psi_{qs} I_{dr} - \psi_{ds} I_{qr}) \tag{3}$$

C_r is the load torque, Ω is the mechanical rotor speed, J is the inertia, f is the viscous friction coefficient, and p is the number of pole pairs.

The stator side active and reactive powers are defined as:

$$\begin{cases} P_s = \frac{3}{2}(V_{ds} I_{ds} + V_{qs} I_{qs}) \\ Q_s = \frac{3}{2}(V_{qs} I_{ds} - V_{ds} I_{qs}) \end{cases} \tag{4}$$

In order to develop a decoupled control of the stator active and reactive powers, we use a Park reference frame linked to the stator flux (Figure 1) [7]. By supposing that the d-axis is oriented along the stator flux position and based on Eq. (1), neglecting R_s we can write:

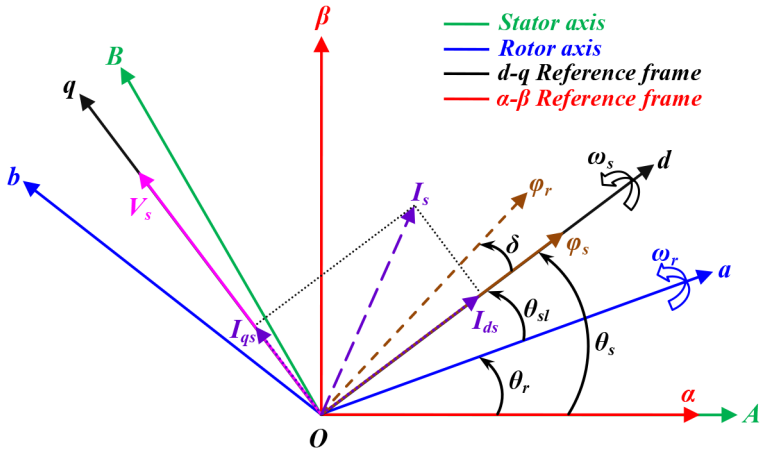

Figure 1. Field oriented control technique.

$$\psi_{ds} = \psi_s \text{ and } \psi_{qs} = 0 \tag{5}$$

$$\begin{cases} V_{ds} = 0 \\ V_{qs} = \omega_s \psi_s \end{cases} \tag{6}$$

$$\begin{cases} I_{ds} = -\frac{M}{L_s} I_{dr} + \frac{\psi_s}{L_s} \\ I_{qs} = -\frac{M}{L_s} I_{qr} \end{cases} \tag{7}$$

By using Eqs. (5), (6), and (7), Eq. (4) can be written as follows:

$$\begin{cases} P_s = -\frac{3}{2}\frac{\omega_s \psi_s M}{L_s} I_{qr} \\ Q_s = -\frac{3}{2}\left(\frac{\omega_s \psi_s M}{L_s} I_{dr} - \frac{\omega_s \psi_s^2}{L_s}\right) \end{cases} \tag{8}$$

The electromagnetic torque can then be expressed by:

$$C_{em} = -\frac{3}{2} p \frac{M}{L_s} I_{qr} \psi_{ds} \tag{9}$$

3. Second order continuous sliding mode control

The chattering phenomenon, which represents a big problem of the standard sliding mode control, can cause harmful effects on the generator because discontinuous control can cause overheating of the coils and excite some unmodeled high frequency dynamics [23]. Some solutions were proposed to avoid this drawback [24,25]. The major idea was to adjust the dynamics in a small region of the discontinuity surface to evade real discontinuity and at the same time to conserve the major characteristics of the whole system. Newly proposed, the high order sliding mode (HOSM) generalizes the essential sliding mode idea that acts on the high order time derivatives of the system deviation from the constraint instead of influencing the first deviation derivative as happens in standard sliding modes [26,27]. In addition to maintaining the major benefits of the original technique, it addresses the chattering effect and presents superior accuracy in practical implementation. These controllers were employed in many research papers in the last two decades [16,17].

The major difficulty encountered with HOSM algorithm implementations is the augmented needed information. Knowledge of $\dot{S}, \ddot{S}, ..., S^{(n-1)}$ is necessary for the carrying out of an nth order controller. Among all the algorithms proposed for the HOSM, the supertwisting algorithm is an exception, which requires only information on the sliding surface [18]. Consequently, this algorithm has been used for the proposed control strategy. As shown in [19], with this algorithm, the stability can be justified for all SOSM controllers.

Using second order continuous sliding mode control is very suitable because it has the desired characteristics, such as robustness under uncertainties. It can also decrease chattering and provides better transient features than the other high order sliding mode [28].

The used control law applied in this paper is given by the following equation [29]:

$$u(t) = -l_1 |S|^{a_1} sgn(S) \cdots - - l_n \left|S^{(n-1)}\right|^{a_n} sgn(S^{(n-1)}) - v \tag{10}$$

Here, v is defined by Eqs. (11) and (12) and the scalars $a_1, a_2, ..., a_n$ satisfy Eq. (13). In addition, $l_1, l_2, ..., l_n$ are scalar coefficients defined such that the nth order polynomial $p^n + l_n p^{n-1} + \cdots + l_2 p + l_1$ is Hurwitz.

$$v(t) = k \cdot |S|^{1/2} sgn(S) + v_1(t) \tag{11}$$

$$\dot{v}_1(t) = \alpha \cdot sgn(S) \tag{12}$$

$$a_{i-1} = \frac{a_i a_{i-1}}{2a_{i+1} - a_i}, \; i = 2, ..., n \tag{13}$$

Here we have $a_n + 1 = 1$ and $a_n = a$.

3.1. SOCSM-DTC of the DFIG

The SOCSM-DTC goal is to control the torque and the rotor flux magnitude of the DFIG. In the C-DTC, flux is controlled by means of the direct axis voltage V_{dr}, while the torque is controlled by means of the quadrature axis voltage V_{qr}.

The proposed SOCSM-DTC, which is designed to control rotor flux and electromagnetic torque of the DFIG, is shown in Figure 2.

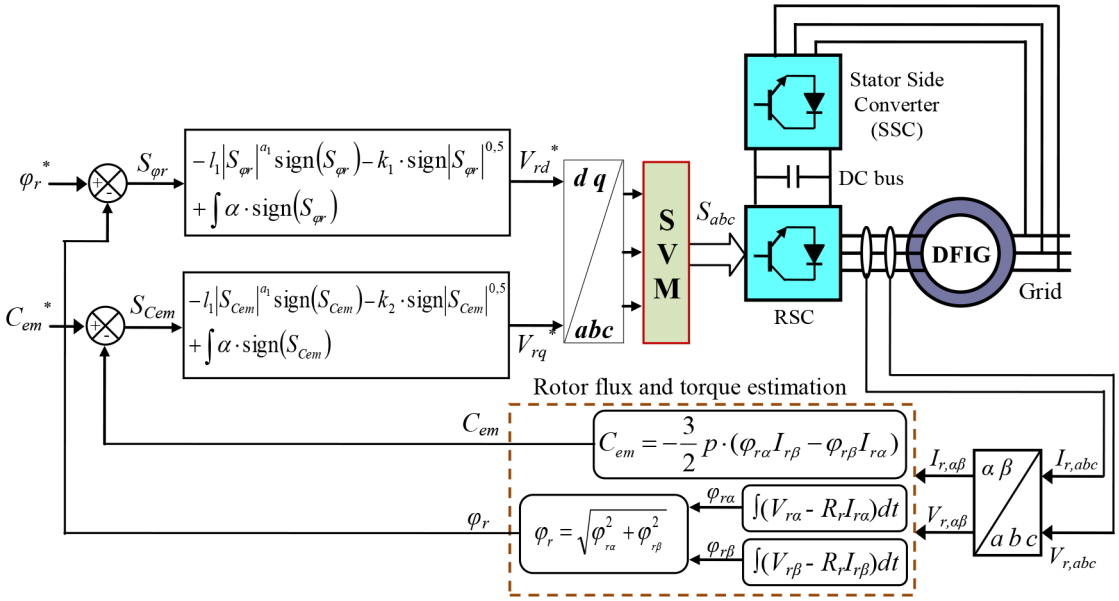

Figure 2. Block diagram of the DFIG with SOCSM-DTC.

The second order continuous sliding mode flux and torque controllers are designed to respectively change the d and q-axis voltages (V_{dr}^* and V_{qr}^*) as in Eqs. (14) and (15).

$$V_{dr}^* = -l_1 \left|S_{\phi r}\right|^{a_1} sign\left(S_{\phi r}\right) - k_1 \cdot sign\left|S_{\phi r}\right|^{1/2} + \int \alpha \cdot sign\left(S_{\phi r}\right) \tag{14}$$

$$V_{qr}^* = -l_1 \left|S_{\phi r}\right|^{a_1} sign\left(S_{Cem}\right) - k_2 \cdot sign\left|S_{Cem}\right|^{1/2} + \int \alpha \cdot sign\left(S_{Cem}\right) \tag{15}$$

Here, the flux magnitude error $S_{\varphi r} = \varphi_r^* - \varphi_r$ and the torque error $S_{Cem} = C_{em}^* - C_{em}$ are the sliding variables, and the constant gains k_1 and k_2 must check the stability conditions.

3.2. Stability and gain choice

Consider a dynamic system with input u, state x, and output y, given by Eq. (16).

$$\frac{dx}{dt} = a(x,t) + b(x,t)u, \quad y = c(x,t) \tag{16}$$

The control difficulty is to discover an input function $u = f(y,\dot{y})$ that can drive the system trajectories to the starting point $y = \dot{y} = 0$ of the phase plane, if possible in a limited time. The input u is defined as a novel state

variable, whereas the switching control is applied to its time derivative, $\dot{u}$. The output y is controlled by a SOCSM controller, with the sliding variable $S = y^* - y$.

This controller does not utilize the derivative of the sliding variable. As imposed by Eqs. (14) and (15), the adequate condition for convergence to the sliding surface and for stability is for the gains to be large enough [14].

$$k_1 > \frac{A_M}{B_m},\ k_2 \geq \frac{4A_M}{B_m^2} \cdot \frac{B_M(K_1 + A_M)}{B_m(K_1 - A_M)} \tag{17}$$

Here, $A_M \geq |A|$ and $B_M \geq B \geq B_m$ are superior and inferior bounds of A and B in the second derivative of y.

$$\frac{d^2y}{dt^2} = A(x,t) + B(x,t)\frac{du}{dt} \tag{18}$$

4. Simulation results and discussions

In this part simulations are carried out with a 1.5 MW DFIG attached to a 398 V/50 Hz

grid, using the environment of MATLAB/Simulink. Parameters of the machine are given in the Table. Both control strategies, C-DTC and SOCSM-DTC, are simulated and compared regarding reference tracking, stator current harmonics distortion, responsiveness to the rotor speed variation, and robustness against machine parameter variations.

Table. The DFIG parameters.

Parameters	Rated value	Unity
Nominal power	1.5	MW
Stator voltage	398	V
Stator frequency	50	Hz
Number of pairs poles	2	
Stator resistance	0.012	Ω
Rotor resistance	0.021	Ω
Stator inductance	0.0137	H
Rotor inductance	0.0136	H
Mutual inductance	0.0135	H
Inertia	1000	kg m^2
Viscous friction	0.0024	Nm/s

4.1. Reference tracking test

The objective of this test is to study the behavior of both DTC control strategies while the DFIG's speed is maintained at its nominal value. Figures 3–5 show the obtained simulation results. As shown by Figures 3 and 4, for the two DTC control strategies, the torque and rotor flux almost perfectly track their references values.

Moreover, contrary to the C-DTC strategy where the coupling effect between the two axes is apparent, we notice that the SOCSM-DTC guarantees the decoupling between them. On the other hand, Figure 5 shows the harmonic spectra of one phase stator current of the DFIG obtained using the fast Fourier transform technique for both DTC control strategies. It can be clearly observed that the total harmonic distortion (THD) is reduced for SOCSM-DTC (THD = 0.98%) when compared to C-DTC (THD = 2.57%).

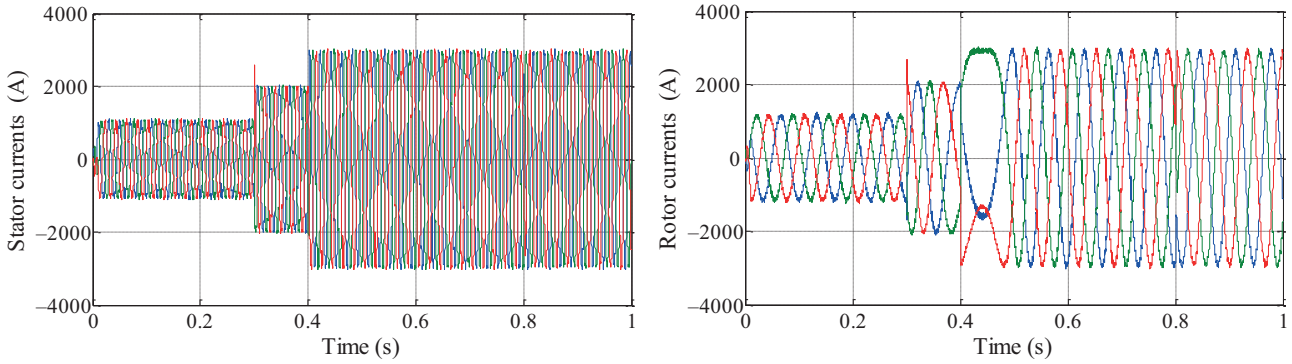

Figure 3. C-DTC strategy responses (reference tracking test).

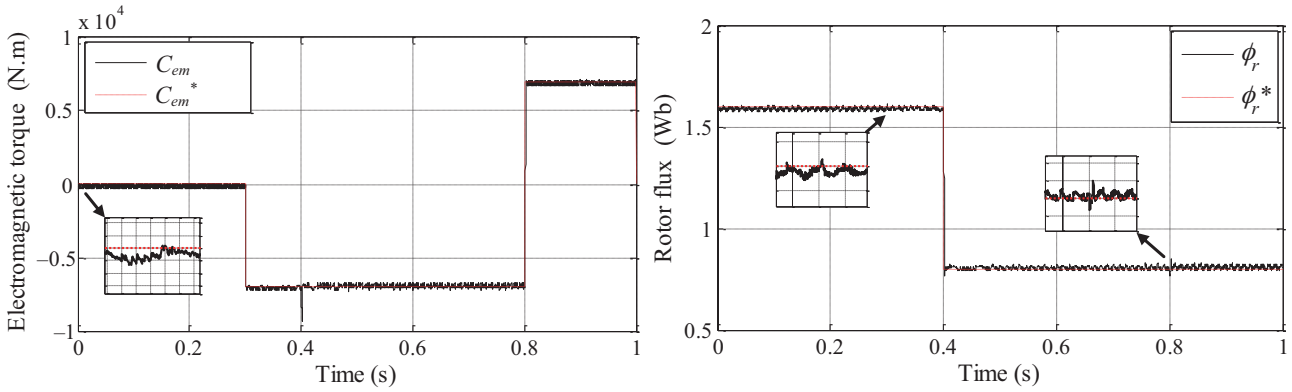

Figure 4. SOCSM-DTC strategy responses (reference tracking test): a) C-DTC, b) SOCSM-DTC.

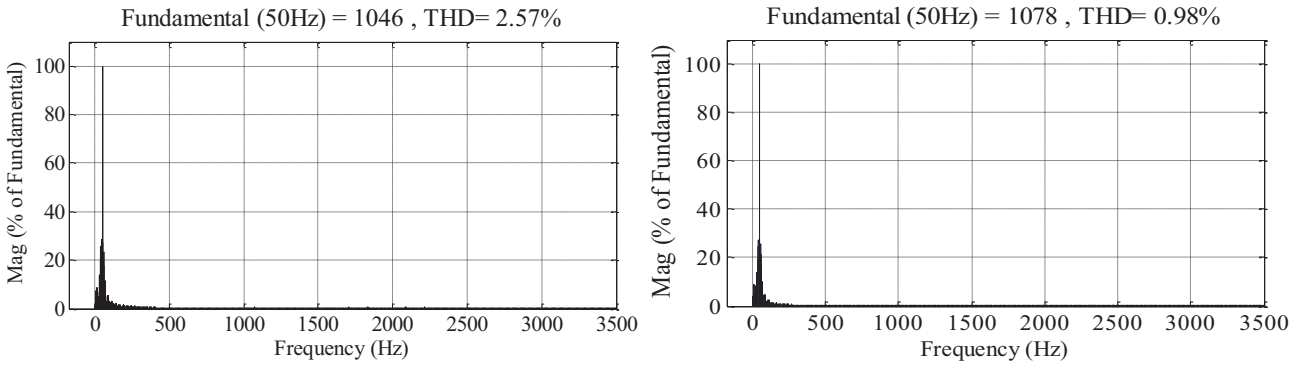

Figure 5. Spectrum harmonic of one phase stator current.

4.2. Sensibility to rotor speed variation

The principle objective of this test is to examine the influence of a mechanical speed variation of the DFIG on electromagnetic torque and rotor flux behaviors for both DTC control strategies. For this object and as shown by Figure 6, the rotor speed was varied in the interval of time $t = 0.4$ s to $t = 0.6$ s from 100 rad/s to 200 rad/s.

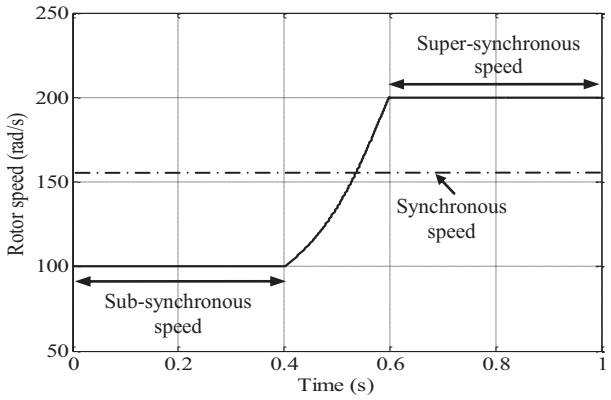

Figure 6. Rotor speed profile.

The simulation results are shown by Figures 7 and 8. These figures show that the speed variation produces a negligible effect on electromagnetic torque and rotor flux curves for both DTC control strategies. This result is attractive for wind energy applications to guarantee stability and quality of the generated power when the speed is changing.

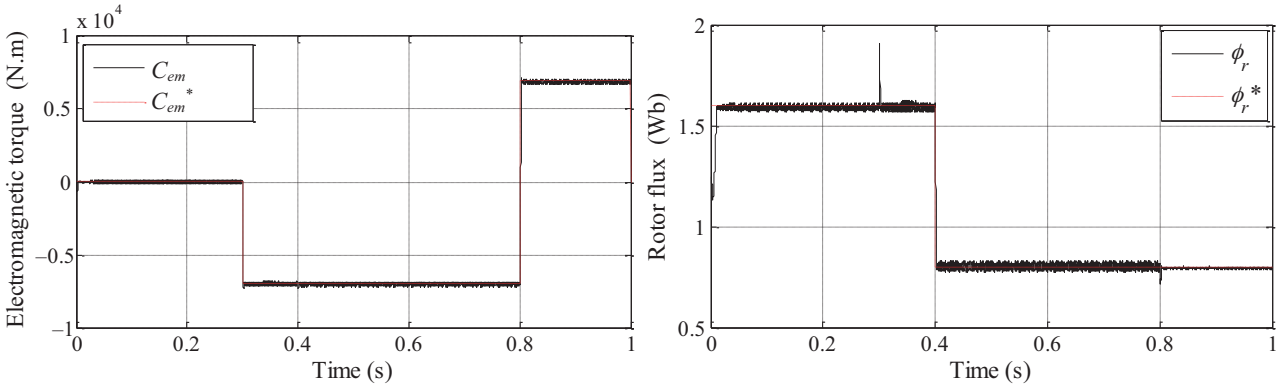

Figure 7. C-DTC strategy responses (sensitivity to the speed variation).

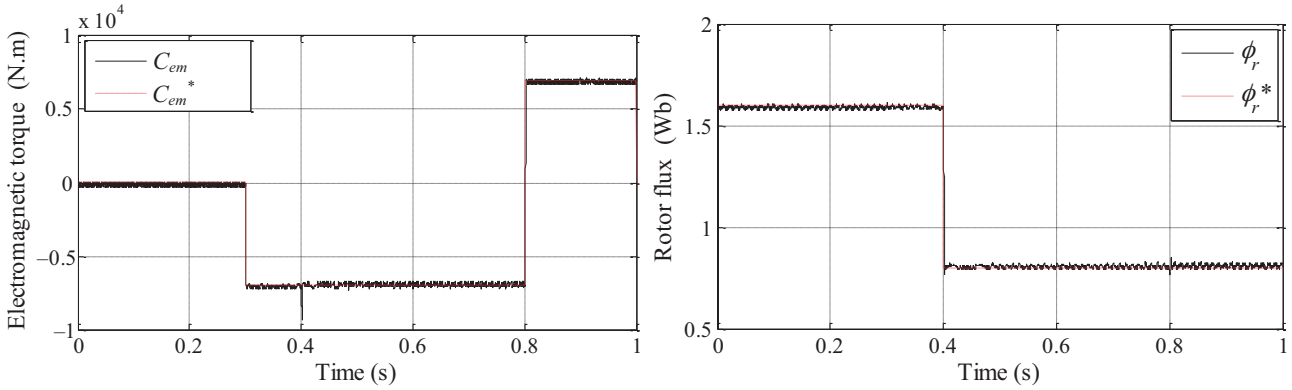

Figure 8. SOCSM-DTC strategy responses (sensitivity to the speed variation).

4.3. Robustness test

For analyzing the robustness of the used DTC control strategies, the machine parameters have been intentionally changed; the values of the stator and the rotor resistances R_s and R_r are doubled and the values of inductances

L_s, L_r, and M are divided by 2. The machine is running at its nominal speed. Simulation results are presented in Figures 9–11. As shown by these figures, parameter variations of the DFIG slightly increase the time-response of the C-DTC strategy. On the other hand, these variations present a clear effect on the torque and flux curves and the effect appears more important for C-DTC than for SOCSM-DTC. Thus, it can be concluded that the proposed SOCSM-DTC strategy is more robust than the C-DTC one.

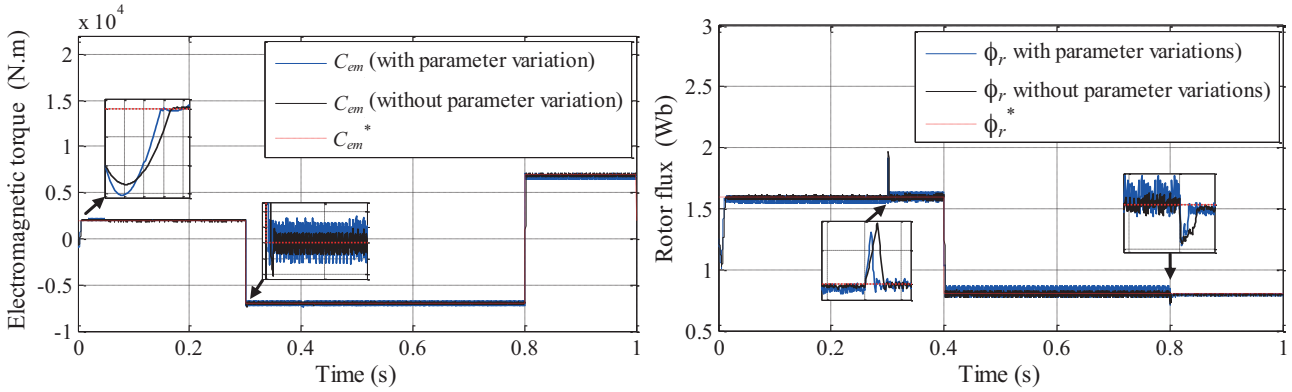

Figure 9. C-DTC strategy responses (robustness test).

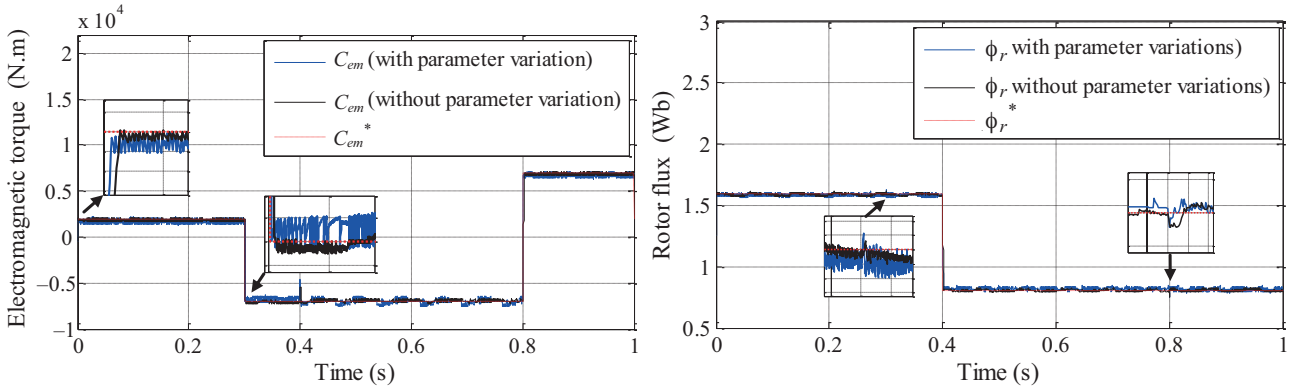

Figure 10. SOCSM-DTC strategy responses (robustness test).

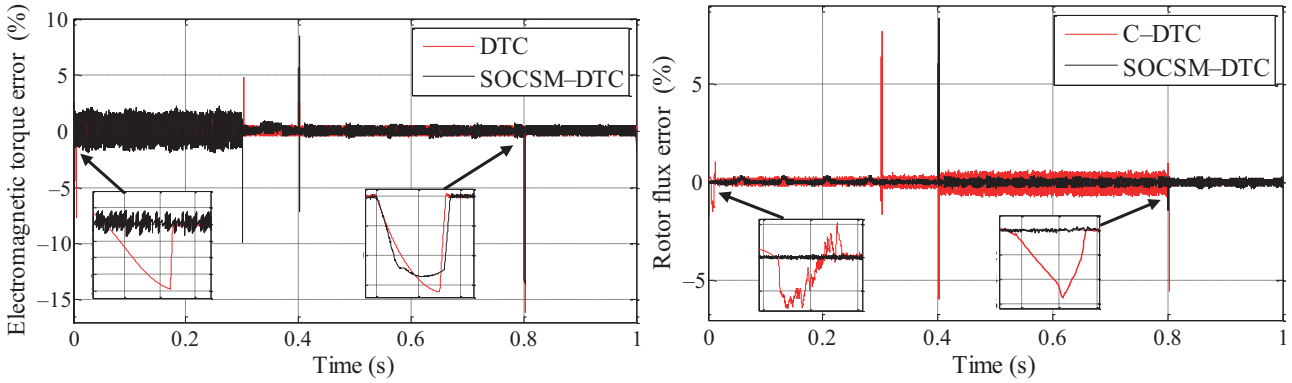

Figure 11. Error curves (robustness test).

5. Conclusion

A novel DTC strategy of a DFIG connected directly to the grid by the stator side and fed by an SVM converter from the rotor side has been presented in this article. As a first step, we started with a study of modeling on the DFIG. Integrated in a WTS, this machine has many advantages as well as variable speed operation and the capability of operation in four quadrants.

In the second step, we adopted a vector control strategy in order to independently control stator active and reactive powers exchanged between the DFIG and the grid. In a third step the SOCSM-DTC was synthesized and compared to the C-DTC. Regarding reference tracking with a DFIG in ideal conditions, both DTC strategies track their references almost perfectly, but a coupling effect appears in the C-DTC responses, which is eliminated in the SOCSM-DTC ones. On the other hand, simulation results have confirmed that the proposed SOCSM-DTC operates with a very lower chattering phenomenon. When the machine's speed is changed, the impact on the torque and rotor flux curves is almost negligible for both DTC strategies. A robustness test has also been investigated where the DFIG parameters have been intentionally modified. These changes induce some disturbances on the torque and flux responses but with an effect almost doubled with the C-DTC strategy compared to that with SOCSM-DTC. Based on all these results it can be concluded that a robust control method such as SOCSM-DTC can be a very attractive solution for devices using DFIG such as wind energy conversion systems.

References

[1] Edrah M, Lo KL, Anaya-Lara O. Impacts of high penetration of DFIG wind turbines on rotor angle stability of power systems. IEEE T Sustain Energ 2015; 6: 759-766.

[2] Ahmed T, Nishida K, Nakaoka M. A novel stand-alone induction generator system for AC and DC power applications. IEEE T Ind Appl 2007; 43: 1465-1474.

[3] Chen SZ, Cheung NC, Wong KC, Wu J. Integral variable structure direct torque control of doubly fed induction generator. IET Renew Power Gen 2011; 5: 18-25.

[4] Rao AM, Kumar NK, Sivakumar K. A multi-level inverter configuration for 4n pole induction motor drive by using conventional two-level inverters. In: IEEE 2015 International Conference on Industry Technology; 17–19 March 2015; Seville, Spain. New York, NY, USA: IEEE. pp. 592-597.

[5] Ardjoun S E, Abid M. Fuzzy sliding mode control applied to a doubly fed induction generator for wind turbines. Turk J Electr Eng Co 2015; 23: 1673-1686.

[6] Yao X, Jing Y, Xing Z. Direct torque control of a doubly-fed wind generator based on grey-fuzzy logic. In: International Conference on Mechatronics and Automation; 2007; Harbin, China. pp. 3587-3592.

[7] Buja GS, Kazmierkowski MP. Direct torque control of PWM inverter-fed AC motors - a survey. IEEE T Ind Electron 2004; 51: 744-757.

[8] Holtz J. Pulse width modulation for electronic power conversion. P IEEE 1994; 82: 1194-1214.

[9] Chen SZ, Cheung NC, Wong KC, Wu J. Integral sliding-mode direct torque control of doubly-fed induction generators under unbalanced grid voltage. IEEE T Energy Conver 2010; 25: 356-368.

[10] Zhu X, Liu S, Wang Y. Second-order sliding-mode control of DFIG-based wind turbines. In: IEEE 2014 3rd Renewable Power Generation Conference; 24–25 September 2014; Naples, Italy. New York, NY, USA: IEEE. pp. 1-6.

[11] Morsy MAA, Said M, Moteleb A, Dorrah HT. Design and implementation of fuzzy sliding mode controller for switched reluctance motor. In: IEEE 2008 International Conference on Industrial Technology; 21–24 April 2008; Chengdu, China. New York, NY, USA: IEEE. pp. 1367-1372.

[12] Yan Z, Jin C, Utkin VI. Sensorless sliding-mode control of induction motors. IEEE T Ind Electron 2000; 47: 1286-1297.

[13] Lascu C, Boldea I, Blaabjerg F. Variable-structure direct torque control – A class of fast and robust controllers for induction machine drives. IEEE T Ind Electron 2004; 51: 785-792.

[14] Lascu C, Blaabjerg F. Super-twisting sliding mode direct torque control of induction machine drives. In: IEEE 2014 Energy Conversion Congress and Exposition; 14–18 September 2014; Pittsburgh, PA, USA. New York, NY, USA: IEEE. pp. 5116-5122.

[15] Benelghali S. On multiphysics modeling and control of marine current turbine systems. PhD, Bretagne Occidentale University, Brest, France, 2009.

[16] Mefoued S. A second order sliding mode control and a neural network to drive a knee joint actuated orthosis. Neurocomputing 2015; 155: 71-79.

[17] Bartolini G, Ferrara A, Usani E. Chattering avoidance by second-order sliding mode control. IEEE T Automat Contr 1998; 43: 241-246.

[18] Levant A, Alelishvili L. Integral high-order sliding modes. IEEE T Automat Contr 2007; 52: 1278-1282.

[19] Levant A. Higher-order sliding modes, differentiation and output feedback control. Int J Control 2003; 76: 924-941.

[20] Levant A. Quasi-continuous high-order sliding-mode controllers. In: Proceedings of the 42nd IEEE Conference on Decision and Control; December 2003; Lahaina, HI, USA. New York, NY, USA: IEEE. pp. 4605-4610.

[21] Kahla S, Soufi Y, Sedraoui M, Bechouat M. On-Off control based particle swarm optimization for maximum power point tracking of wind turbine equipped by DFIG connected to the grid with energy storage. Int J Hydrogen Energ 2015; 40: 13749-13758.

[22] Bakouri A, Abbou A, Mahmoudi H, Elyaalaoui K. Direct torque control of a doubly fed induction generator of wind turbine for maximum power extraction. In: IEEE International Renewable and Sustainable Energy Conference; 17–19 October 2014; Morocco. New York, NY, USA: IEEE. pp. 334-339.

[23] Wang WJ, Chen JY. Passivity-based sliding mode position control for induction motor drives. IEEE T Energy Conver 2005; 20: 316-321.

[24] Emelyanov SV, Korovin SK. Applying the principle of control by deviation to extend the set of possible feedback types. Soviet Physics Doklady 1981; 26: 562-564.

[25] Slotine JJE. Sliding controller design for nonlinear systems. Int J Control 1984; 40: 421-434.

[26] Beltran B, Benbouzid MEH, Ahmed-Ali T. High-order sliding mode control of a DFIG-based wind turbine for power maximization and grid fault tolerance. In: IEEE 2009 International Electric Machines and Drives Conference; May 2009; Miami, FL, USA. New York, NY, USA: IEEE. pp. 183-189.

[27] Beltran B, Benbouzid MH, Ahmed-Ali T. Second-order sliding mode control of a doubly fed induction generator driven wind turbine. IEEE T Energy Conver 2012; 27: 261-269.

[28] Levant A. Quasi-continuous high-order sliding-mode controllers. IEEE T Automat Contr 2005; 50: 1812-1816.

[29] Edwards C, Shtessel Y. Adaptive continuous higher order sliding mode control. In: 19th World Congress, the International Federation of Automatic Control; 24–29 August 2014; Cape Town, South Africa. pp. 10826-10831.